eLIFE
elifesciences.org

Figures and figure supplements

Symmetric exchange of multi-protein building blocks between stationary focal adhesions and the cytosol

Jan-Erik Hoffmann, et al.

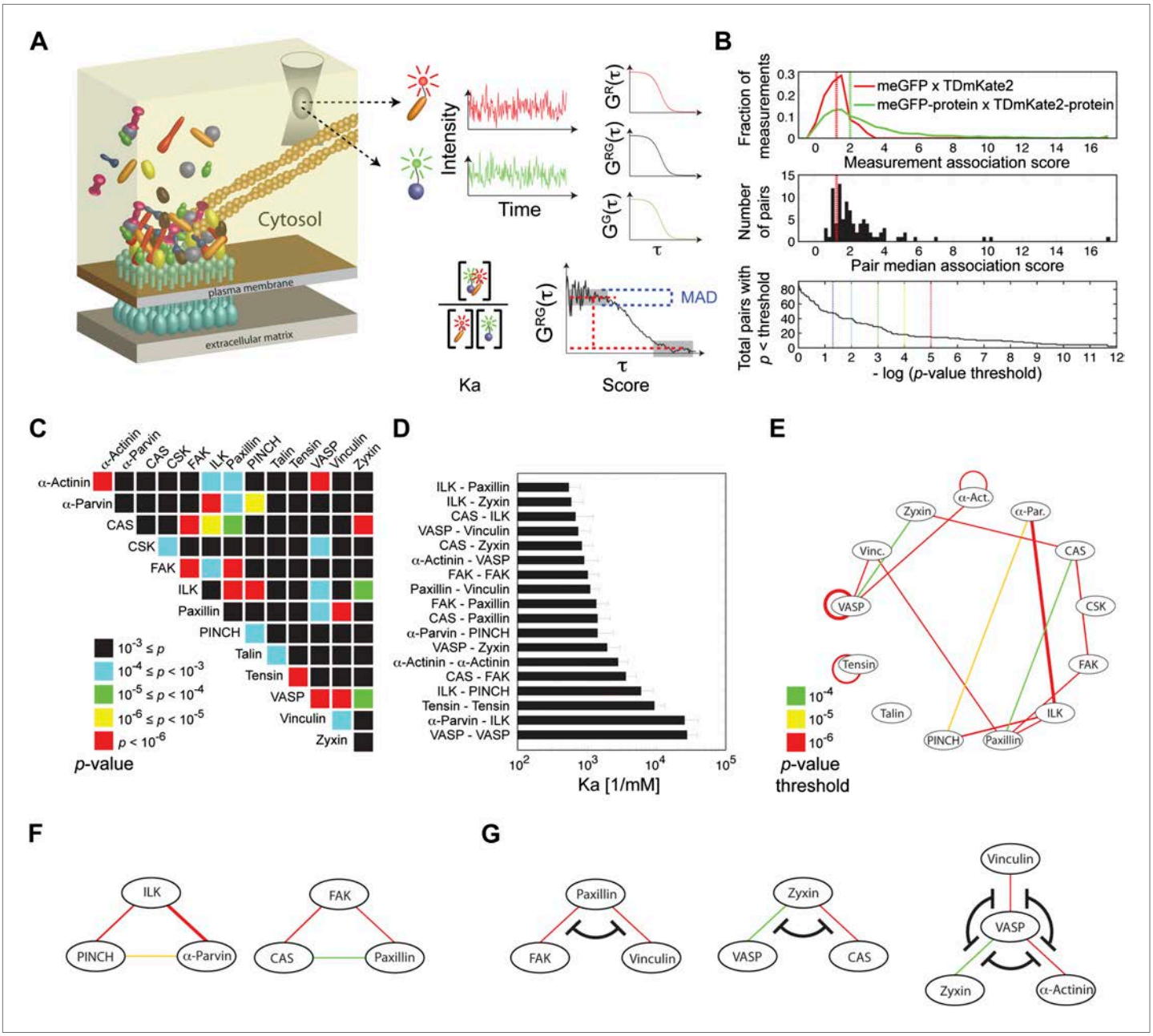

Figure 1. Extensive physical associations between components of cell-matrix adhesion sites in the cytosol. (**A**) Pairwise physical associations between proteins tagged with meGFP and TDmKate2 were measured in the cytosol of REF52 and NIH3T3 cells using FCCS (schematized). From these measurements the apparent association constants (*Ka*) and the association scores were derived as described. (**B**) Top, area-normalized distributions of association scores between meGFP and TDmKate2 alone (i.e., negative control, $n = 126$ cells, red line) and between the different analyzed components of adhesion sites in all individual valid measurements performed in REF52 cells ($n = 1914$ cells; green line) with their corresponding medians (vertical lines). Middle, the distribution of median association score of the 91 protein pairs ($60 \geq n \geq 9$ cells per each pair). Red line indicates the median association score of the negative control. Bottom, the total number of pairs with a median association score bigger than that of the negative control at different statistical confidences (***Supplementary file 1***). The p-values indicate the probability that the observed median association score of a given pair is bigger than that of the negative control by coincidence. Thus a higher −log(p-value threshold) value means a higher statistical confidence for physical association. (**C**) A heatmap indicating the p-value of each protein pair in REF52 cells. (**D**) A bar plot showing the median ± median absolute deviation (MAD) *Ka* for protein pairs having p-value <0.0001 ($n \geq 13$ cells per pair). (**E**) The network of physical associations between the analyzed proteins. Shown edges are those having p-value <0.0001 in REF52 and p-value <0.02 in NIH3T3 (***Supplementary file 1***). Edges color and width indicate p-value categories as in (**C**) and proportionally *Ka* in REF52, respectively. (**F**) Based on the network shown in (**E**), two potential ternary complexes are

Figure 1. Continued on next page

Figure 1. Continued

indicated. (**G**) Mutually exclusive physical associations inferred from (**D**) and (**E**) as cases in which two or more proteins exhibit pairwise associations with another protein but not between themselves.

DOI: 10.7554/eLife.02257.003

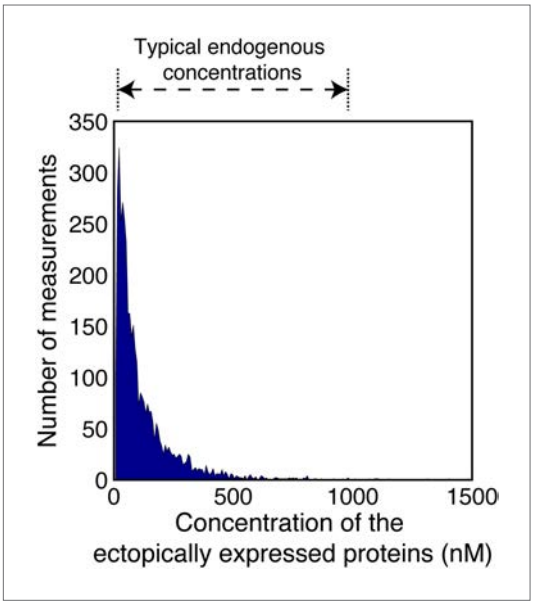

Figure 1—figure supplement 1. Concentrations of the ectopically expressed proteins in the FCCS measured cells.

DOI: 10.7554/eLife.02257.004

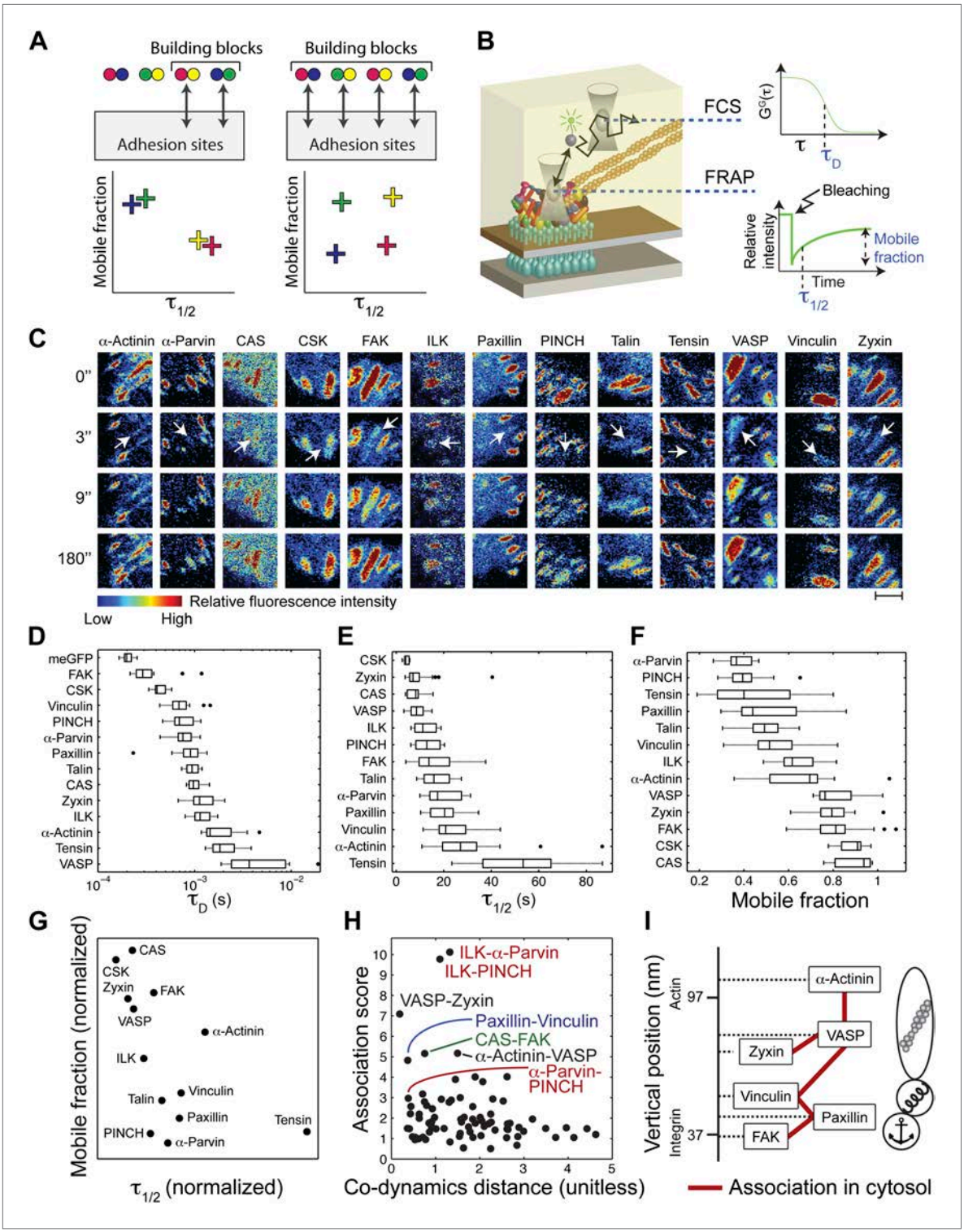

Figure 2. The cytosolic building blocks of cell-matrix adhesion sites are combinatorially diversified. (**A**) Not all cytosolic integrin-adhesome complexes are necessarily building blocks for adhesion sites. If each protein is in only one type of building blocks then physically associated proteins should exhibit the same dwell times ($\tau_{1/2}$) and mobile fractions in focal adhesions. (**B**) REF52 cells expressing the analyzed proteins tagged with meGFP were measured using FRAP and FCS to quantify their $\tau_{1/2}$ and mobile fractions in focal adhesions and their dwell times in a confocal volume in the cytosol (τ_D). (**C**) Example FRAP images before (0") and after bleaching a focal adhesion (arrows). Scale bar, 5 μm. (**D**–**F**) Box plots of the τ_D (26 ≥ n ≥ 14 cells), $\tau_{1/2}$ and mobile fractions (31 ≥ n ≥ 7 cells) of each protein. (**G**) Median $\tau_{1/2}$ vs median mobile fraction of each protein normalized to zero-mean and unit-variance. Thus, in this plot the Euclidean distance (co-dynamics distance) between proteins quantifies the difference in their dynamics. (**H**) The co-dynamics

Figure 2. Continued on next page

Figure 2. Continued

distance vs median association score of all possible 78 heteromeric protein pairs. (**I**) The reported vertical distance from substrate of 6 of the analyzed components across focal adhesions (***Kanchanawong et al., 2010***) and the cytosolic associations between them as measured here (***Figure 1E***). Anchor, spring, and actin symbols indicate vertical layers of integrin signalling, mechanosensing and actin regulation across focal adhesions, respectively (***Kanchanawong et al., 2010***).

DOI: 10.7554/eLife.02257.005

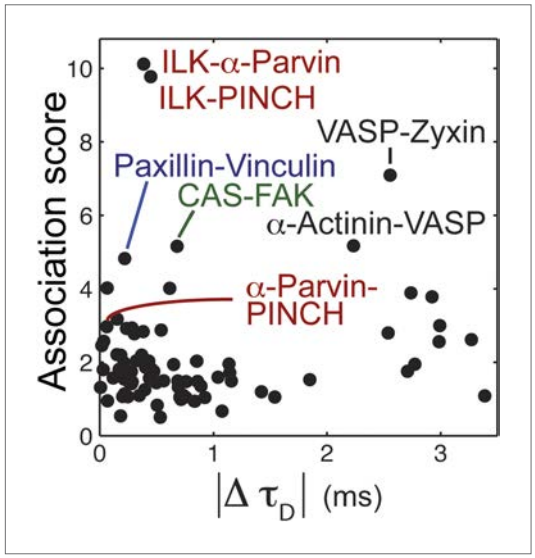

Figure 2—figure supplement 1. The relation between physical associations and similarity in diffusion speeds in the cytosol.

DOI: 10.7554/eLife.02257.006

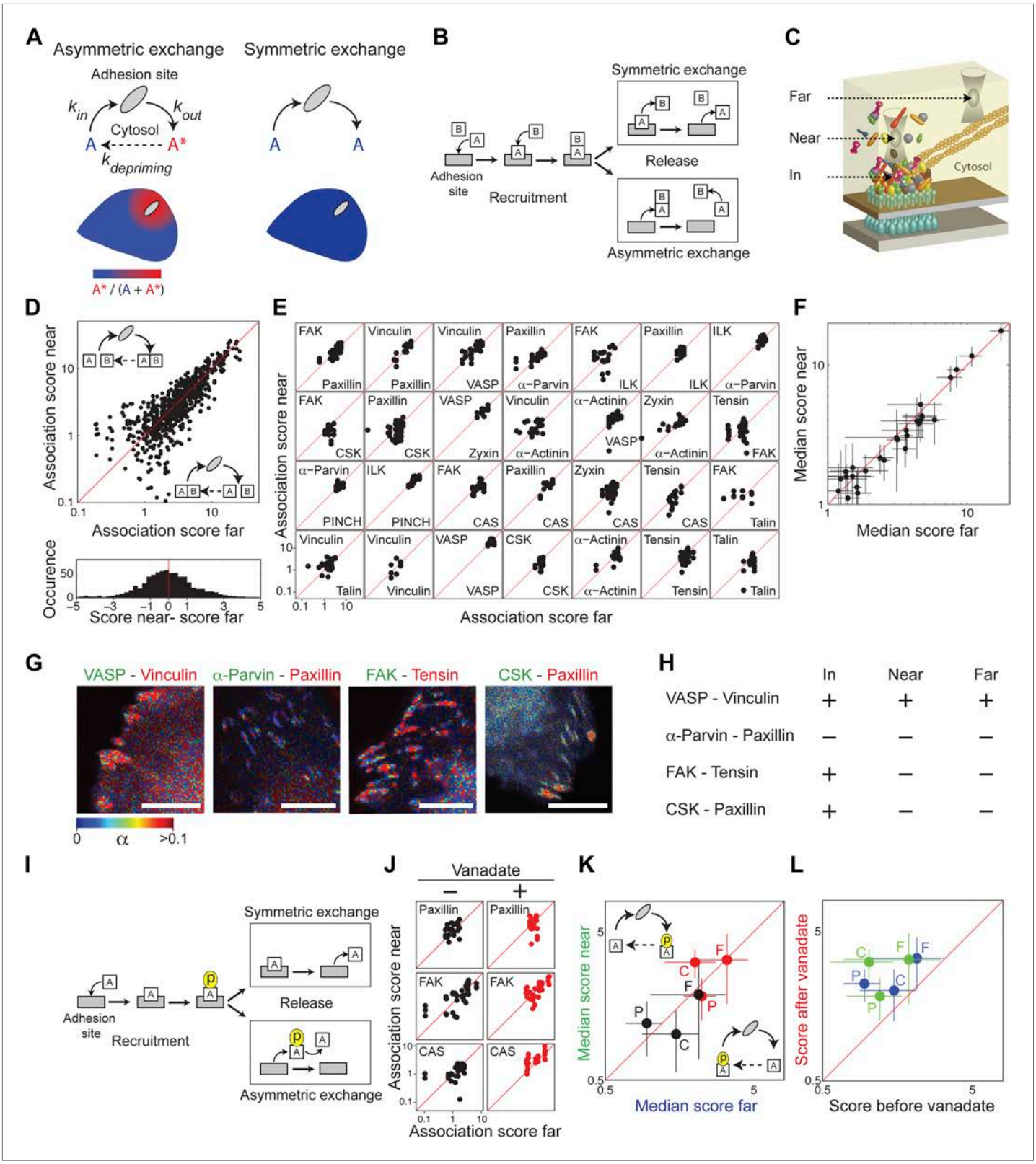

Figure 3. Symmetric material exchange between stationary focal adhesions and cytosol. (**A**) The symmetric and asymmetric models of material exchange between adhesion sites and cytosol. In symmetric exchange a component, *A*, exits from adhesion site in the same state it had upon entering to it. In asymmetric exchange *A* exits in a different, primed state *A** and relaxes back to state *A* in the cytosol, thereby generating a spatial gradient of the primed state emanating from adhesion sites. (**B**) Formulation of the two models for the case in which priming (of *A*) is based on interaction

Figure 3. Continued on next page

Figure 3. Continued

(with protein *B*). Here, asymmetric exchange would generate a spatial gradient of *AB* complex concentration emanating from adhesion sites. (**C**–**F**) Discriminating between the two models by measuring the physical associations near (<1.5 μm) and far from focal adhesions for 28 protein pairs as named in (**E**). Scatter plots compare the association scores near vs far from focal adhesions for all the 28 pairs together (n = 755 focal adhesions) (**D**), for each pair separately ($n \geq 9$) (**E**) or for the median score of each pair ± MAD (**F**). Data-points far from the equality diagonals (dashed red lines) would correspond to asymmetric exchanges, as illustrated in (**D**), while data-points along the diagonal indicate symmetric exchange. Histogram in (**D**) shows the distribution of the difference in association scores near and far from focal adhesions. (**G**) FLIM images color-coding the fraction, α, of donor- (mCitrine-) tagged protein (green) that FRETs to the acceptor- (mCherry-) tagged protein (red) for four protein pairs. Scale bars, 10 μm. (**H**) Comparison of the interaction states of the four protein pairs shown in (**G**) in focal adhesions with their physical associations near and far from focal adhesions. (**I**) Formulation of the symmetric and asymmetric models for the case in which priming is based on phosphorylation. (**J**–**L**) Scatter plots comparing the association scores of meGFP-dSH2 with paxillin, FAK, and CAS (denoted P, F, and C, respectively) near vs far from focal adhesions (green and blue, respectively) and before vs after vanadate treatment (black and red, respectively). Error bars indicate MAD ($n \geq 23$ focal adhesions).

DOI: 10.7554/eLife.02257.007

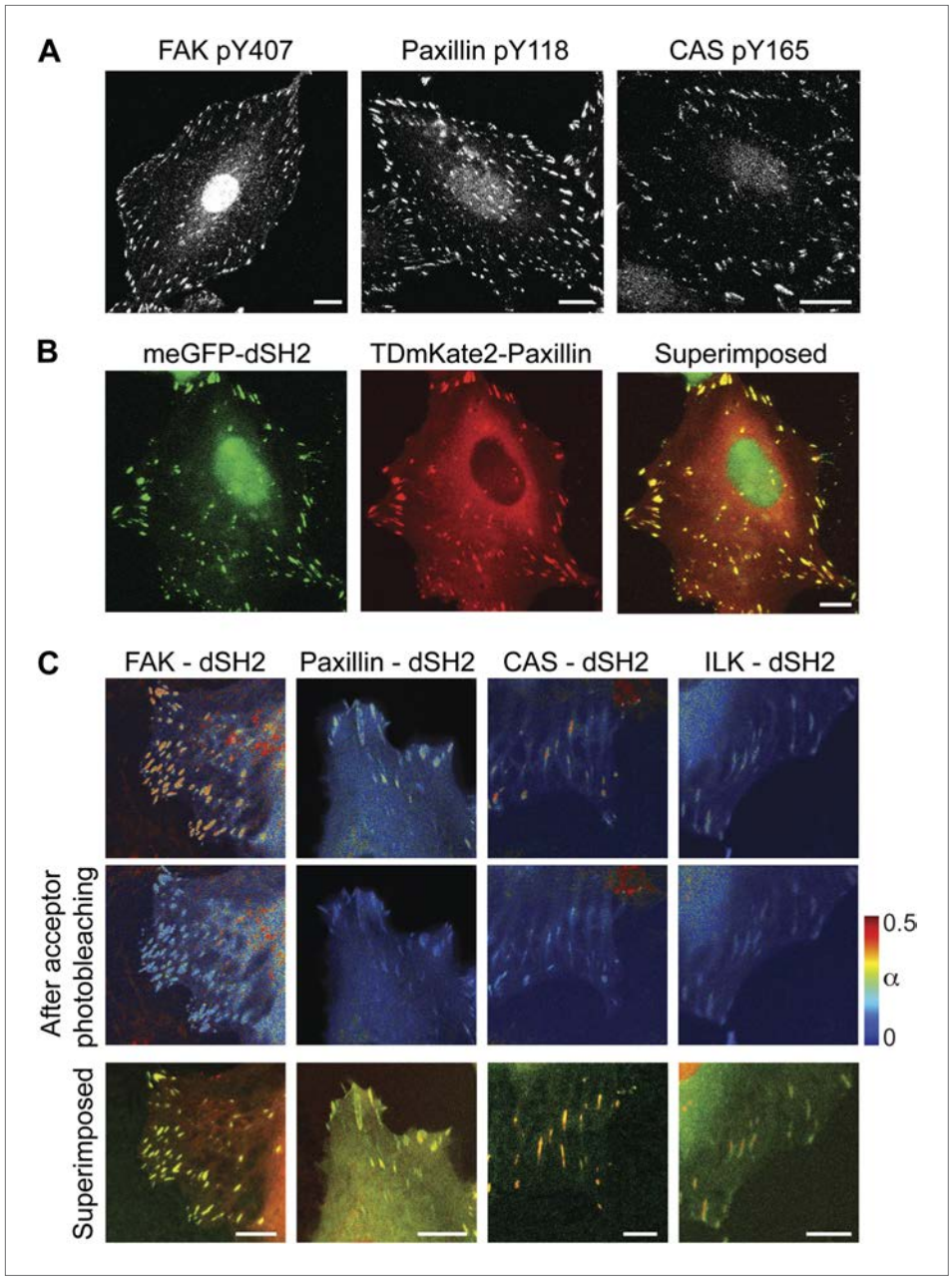

Figure 3—figure supplement 1. FAK, paxillin, and CAS are tyrosine-phosphorylated and interact with SH2 domain in focal adhesions.

DOI: 10.7554/eLife.02257.008

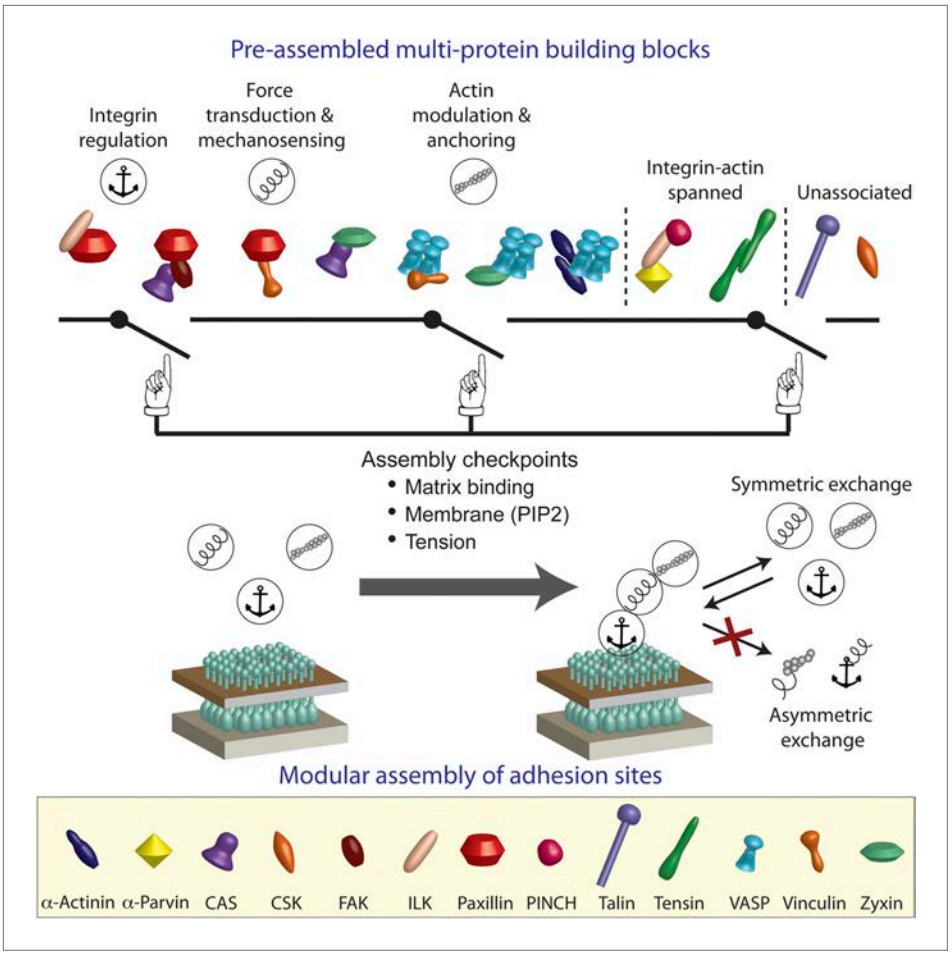

Figure 4. A model of switchable formation of adhesion sites via pre-assembled multi-protein building blocks. The integrin adhesome is pre-assembled in the cytosol as multi-protein building blocks for adhesion sites. These building blocks are combinatorially diversified but confined in their size. Most of the building blocks form modules that are consistent with the previously reported (***Kanchanawong et al., 2010***) vertical continuum of anchoring, mechanosensing, and actin regulation layers across focal adhesions. In the cytosol, the pre-assembled building blocks cannot further assemble to form bigger structures due to mutual exclusiveness between protein interactions and allosteric regulations. On the plasma membrane, the system can get locally switched on to assemble an adhesion site by passing through checkpoints that enable additional protein interactions in the integrin adhesome. These checkpoints include anchoring of integrins to the extracellular matrix, mechanical stretching of proteins like talin and CAS by actomyosin contractility, and activation of proteins like vinculin and talin by PIP2 on the plasma membrane. Symmetric material exchange between adhesion sites and cytosol retains the wiring of the building blocks and therefore retains the assembly logic and switchability of the system.

DOI: 10.7554/eLife.02257.009